Charge Transfer and Dissociation in Collisions of Metal Clusters with Atoms

C. Bréchignac,[1] Ph. Cahuzac,[1] B. Concina,[1] J. Leygnier,[1] L. F. Ruiz,[2] B. Zarour,[3]
P. A. Hervieux,[4] J. Hanssen,[4] M. F. Politis,[5] and F. Martín[2]

[1]*Laboratoire Aimé Cotton, C.N.R.S., Bâtiment 505, Université Paris Sud, 91405 Orsay cedex, France*
[2]*Departamento de Química, C-9, Universidad Autónoma de Madrid, 28049 Madrid, Spain*
[3]*Max-Planck-Institut für Physik Komplexer Systeme, Nöthnitzer Strasse 38, 01187 Dresden, Germany*
[4]*L.P.M.C., Institut de Physique, Technopôle 2000, 57078 Metz, France*
[5]*G.P.S., Université Paris 7, 2 Place Jussieu 75251 Paris cedex 05, France*

We present a combined theoretical and experimental study of charge transfer and dissociation in collisions of slow Li_{31}^{2+} clusters with Cs atoms. We provide a direct quantitative comparison between theory and experiment and show that good agreement is found only when the exact experimental time of flight and initial cluster temperature are taken into account in the theoretical modeling. We demonstrate the validity of the simple physical image that consists in explaining evaporation as resulting from a collisional energy deposit due to cluster electronic excitation during charge transfer.

Charge transfer (CT) occurs in numerous physical and chemical processes involving atomic, molecular, or biological species and surfaces. The fundamental aspects of CT have been thoroughly investigated in atomic and molecular systems since the early days of quantum mechanics, while surfaces have recently entered the scene in connection with technological applications. The study of CT with clusters has received much less attention.

The available experimental methods allow one to selectively prepare metal clusters of almost any size. Thus, metal clusters are the ideal tool to bridge the gap between molecules and surfaces. A singular aspect of CT in cluster-atom collisions is that it competes with electron excitation and dissociation even at low impact energy [1–3]. This makes experiments difficult to analyze and is a challenge for theoretical models, which, among the large number of electronic and nuclear degrees of freedom (DOF), have to uncover the relevant ones (see [2,4–7] and references therein). As a consequence, rigorous attempts to confront theory and experiment at a quantitative level are very scarce. One of these attempts has been the study of CT in $Na_9^+ +$ Cs collisions [8–12], for which the theory [11] has provided absolute CT cross sections in good agreement with those deduced from experiment [8].

To understand the complexity of the problem, we must recall that CT leads to evaporation of one or several fragments. Thus, a direct comparison between theory and experiment is possible only for the relative intensities of the cluster fragments (the observables). As the theoretical work on $Na_9^+ +$ Cs [12] has shown, this comparison is not straightforward. The latter work suggests that evaporation cross sections critically depend on the initial cluster temperature T and the experimental time-of-flight (TOF) window τ_e. While the TOF can be accurately determined in most experiments, the initial temperature is known only indirectly. In fact, temperature is evenly distributed in a finite interval [13,14] which, for small Li and Na clusters, may be as large as 200–1200 K.

The aim of this Letter is to provide a deeper insight on the relation between CT and evaporation by choosing a system in which the various experimental conditions can be strictly controlled. We report on results of a combined experimental and theoretical study of CT and evaporation in collisions of slow Li_{31}^{2+} clusters with Cs atoms. The advantage of choosing this system is threefold. First, alkali clusters are among the best known clusters. Second, while CT leads to neutral species when singly charged clusters are used, CT products in the present experiment are also charged and, therefore, evaporative fragments can be easily detected and identified by mass spectrometry. Third, the size of the chosen cluster is larger than its critical value for Coulomb fission [15]; thus, Li_{31}^{2+} clusters are produced quite abundantly and with a relatively narrow temperature distribution, 420 ($\pm$50)–660 ($\pm$50) K (see below).

We start by briefly describing the experimental setup (see details in [1,13,16]). A distribution of neutral Li clusters is generated by a gas aggregation source. They are ionized within the multigrid acceleration device of a tandem Wiley-Mc-Laren TOF mass spectrometer by a 10 ns pulsed KrF excimer laser at a photon energy of 5 eV (Fig. 1). The laser intensity is large enough to (multi)ionize, photoexcite, and warm the clusters during the pulse duration. Rapid sequential evaporation occurs during the residence time ($\simeq 1~\mu$s) in the ionizing region, which shifts down to lower masses the initial cluster distribution. Under these conditions, clusters entering the TOF constitute an "evaporative ensemble" [14] with a temperature distribution that depends on the experimental time windows. The ion kinetic energy is determined by the accelerating voltage V_0, which is varied from 2 to 8 kV. In the first drift tube of the TOF, the clusters are
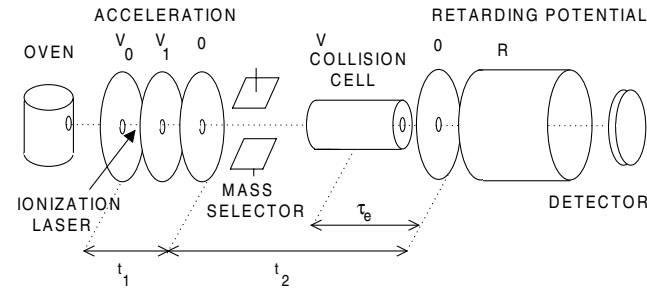
FIG. 1. Experimental setup. Li_{31}^{2+} clusters are produced and mass selected, then interact with a vapor. The collision products are charge and mass analyzed at t_2 by TOF spectrometry.

selected by an electrostatic gate according to their mass/charge ratio and then cross a 20 cm long collision cell containing (or not) the target. The cell pressure is kept low enough to ensure single collision conditions. Downstream from the cell, but upstream from the second drift tube, a retarding electrostatic potential V_R allows one to separate in time charged and neutral products.

Clusters produced as an evaporative ensemble contain some internal energy. Thus, they partially undergo unimolecular dissociation (UD) during their propagation in the TOF. Under our experimental conditions, UD is dominated by evaporation of a neutral monomer:
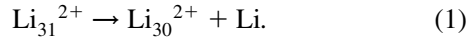
$$Li_{31}^{2+} \rightarrow Li_{30}^{2+} + Li. \quad (1)$$

The dissociation ratio $Li_{30}^{2+}/Li_{31}^{2+}$ depends on the two time windows of the experiment: the residence time in the accelerating region ($t_1 \sim 2.4 \ \mu s$) and the propagation time in the drift tube of the TOF ($t_2 \sim 19 \ \mu s$). Products of the UD process propagate in the first drift tube with the center-of-mass velocity of the parent. They are spatially resolved into individual mass packets in the second drift tube thanks to V_R. They are observed even when the Cs pressure in the collision cell is zero. When the cell is activated, the structure displayed by the retarding field images the combined effects of UD and CT. Thus, by comparing the spectra obtained cell on and cell off, one identifies the signals that are exclusively due to CT.

Figure 2 shows mass spectra corresponding to three values of V_R: 0, 1250, and 2500 V. The atomic density in the cell is $\simeq 2 \times 10^{11}$ at/cm^3. When the potential is switched off, the ion peak contains the residual parent and all the collision products. At the intermediate V_R value, one distinguishes a shouldered peak, whose center of mass corresponds to the singly charged species Li_{30}^+, and a twinned structure which includes the residual Li_{31}^{2+} parent and the Li_{30}^{2+} fragment. The intensity of the shouldered peak varies with the cell pressure and, therefore, it is associated with the singly charged species that is directly produced by CT. In contrast, the relative intensity of the twinned peaks is not sensitive to the cell pressure and so remains for vanishingly low values of the cell pressure. Thus, the twinned peaks are unambiguously
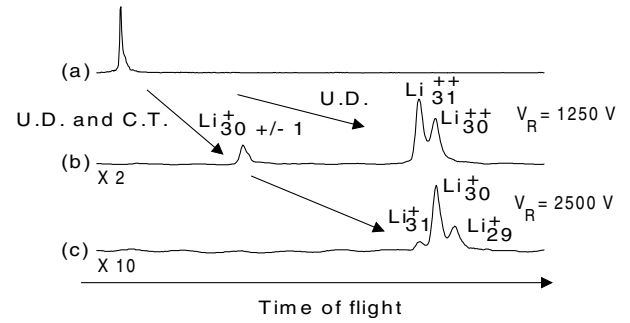

FIG. 2. (a) TOF mass spectrum for Li_{31}^{2+} (no collisions, no electrostatic analysis). (b) TOF charge and mass analysis of the collision products at t_2 for $V_R = 1250$ V. (c) Same as (b) but for $V_R = 2500$ V.

associated with the UD process (1) and not to a collisional induced dissociation process. The increase of V_R increases the mass discrimination and reveals a structure within the singly charged mass peak. It appears now as a distribution of three components identified as Li_{29}^+, Li_{30}^+, and Li_{31}^+, Li_{30}^+ being the dominant peak. Li_{29}^+ and partially Li_{30}^+ result from evaporation associated with CT. The evaporation rate involves a relatively short propagating time τ_e from the collision cell up to the retarding potential plate. This leads us to conclude that CT is accompanied by a significant amount of energy deposit in the cluster ion. As we see later, this energy deposit involves cluster excited states.

Summarizing the observations, the following channels are relevant to deduce the cross sections: (i) CT occurring for both the parent and its UD product [see Eq. (1)]:

$$Li_{31}^{2+} + Cs \rightarrow Li_{31}^+ + Cs^+, \quad (2)$$
$$Li_{30}^{2+} + Cs \rightarrow Li_{30}^+ + Cs^+; \quad (3)$$
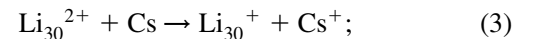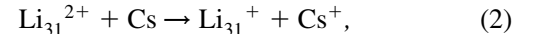
(ii) evaporation of excited singly charged products (the absence of Li_{28}^+ clusters gives a limit to the sequences):

$$Li_{31}^+ \rightarrow Li_{30}^+ + Li \rightarrow Li_{29}^+ + 2Li, \quad (4)$$
$$Li_{30}^+ \rightarrow Li_{29}^+ + Li. \quad (5)$$
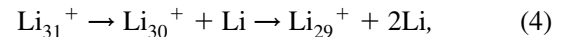
As shown in [8], CT cross sections for medium-size singly charged Li clusters barely depend on cluster size. Therefore, it is reasonable to assume that the cross sections associated with Eqs. (2) and (3) are identical. Thus, we can easily deduce the absolute value of the CT cross section, σ, from Beer's law:

$$1 - \frac{[Li_{31}^+] + [Li_{30}^+] + [Li_{29}^+]}{[Li_{31}^{2+}]^0 + [Li_{30}^{2+}]^0} = \exp(-\sigma n_{at} l), \quad (6)$$

where the denominator contains the parent ion peak intensity before the collision and the numerator the ion peak intensity of the charge exchange products. n_{at} is the atomic vapor density, and l is the length of the collision cell. In order to overcome the uncertainty on

the $n_{at}l$ value, we have used Na^+ projectiles and compared our values with the absolute cross sections of Perel and Daley for the same collisional system and collision energy [17]. We have found $\sigma = 250 \pm 50$ Å^2 for an impact energy of 3 keV. We have checked that, within the experimental uncertainty, the CT cross section barely changes in the energy range 1–4 keV. Similar values have been found when K targets are used. Previous measurements with doubly charged Na clusters led to comparable results, with a slow decrease of the cross section with the collision energy [16]. These values are remarkably larger than those found for singly charged species with the same number of atoms and at the same collisional energy [16].

When the collision cell is off, we observe only UD [see (1)]. Hence, we deduce the initial temperature distribution of Li_{31}^{2+} and Li_{30}^{2+} projectiles by using the evaporative ensemble model of [16]. Here we have improved this model by including anharmonic effects. When the cell is on, the same model allows us to estimate the internal energy δE of the singly charged clusters due to CT (see [13] for details). We have found $\delta E = 1.0 \pm 0.1$ eV.

In addition to the experiment described above, we have carried out theoretical calculations using the method of Refs. [7,12]. This method has been previously used to study CT and fragmentation in $Na_9^+ + Cs$ collisions. Our method benefits from the different time scales associated with the collision and the internal motion of the cluster nuclei: in the first place, because the collision time ($\tau_{col} \sim 10^{-14}$ s) is much shorter than the cluster vibrational period ($\tau_v \sim 10^{-12}$ s) in the range of impact velocities considered in this work ($v \sim 0.01$–0.03 au); in the second place, because the electron-phonon coupling responsible for the observed dissociation has a characteristic lifetime of $\tau_{rel} \sim 10^{-13}$–10^{-12} s and, therefore, can be ignored during the collision. As a consequence, the only relevant nuclear DOF in the CT dynamics is the relative distance R between the impinging cluster and the atomic target. Furthermore, evaporation is a postcollisional effect that can be described separately provided that the collisional energy deposit δE and the initial cluster temperature is known. Still, dissociation may be induced in frontal collisions with the target, but this will not be taken into account because the experiment shows that it is a minor dissociation channel (a similar situation can be found in [10,16]). This is consistent with the fact that evaporation induced by CT occurs at long distances and, therefore, is the dominant process.

According to the above discussion, the collision and the subsequent evaporation process have been treated separately, δE being the connection between these two problems. In a first step, the model treats the collision dynamics using (i) a fully quantum mechanical description of the relevant electronic DOF in the framework of the independent electron model and (ii) the semiclassical impact parameter approach. An additional simplification is the use of the spherical jellium model to represent the

ionic core potential of the cluster. As discussed in [12], this is more realistic than using the lowest-energy geometry of the cluster because, for hot metal clusters, isomerization among different geometries occurs spontaneously and, therefore, an average spherical geometry is closer to the experimental situation. We have used the "molecular close-coupling" formalism to solve the time-dependent Schrödinger equation, which leads immediately to the CT cross section. δE can be easily evaluated from the calculated transition amplitudes to Li_{31}^+ excited states. To obtain the total internal energy of the cluster, one has to add its initial thermal energy. For a given temperature, the latter has been obtained from the experimental curve relating temperature and internal energy of bulk Li [18]. The total internal energy is then used to evaluate the evaporation rate constants in the framework of the microscopic and microcanonical statistical theory of Weisskopf [19]. Dissociation energies of the different Li_n^+ fragments have been taken from experiment [13]. Anharmonic effects are included by employing the level density obtained from the specific entropy of bulk lithium [18]. The calculated rate constants are used to build a system of differential equations that includes both monomer and dimer evaporation as well as sequential evaporation events up to any order. Time integration is performed up to $t = \tau_e$. This leads to branching ratios for the different fragments and, hence, to apparent "partial" cross sections.

In Fig. 3 we compare the total and partial CT cross sections obtained from this model with those determined experimentally. The theoretical partial cross sections have been calculated for $T = 450$ K (i.e., within the evaporative ensemble temperature range $T = 420$–660 K) and $\tau_e = 3$ μs (the TOF in the present experiment). Figure 3 shows good agreement between theory and experiment. In particular, theory
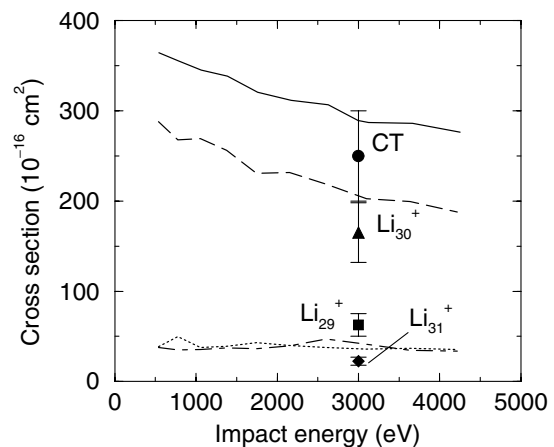

FIG. 3. CT and evaporation cross sections. Symbols with error bars: experiment (valid in the range 1–4 keV); lines: theory. CT: full line and circle; Li_{31}^+: dotted line and diamond; Li_{30}^+: dashed line and triangle; Li_{29}^+: dot-dashed line and square.
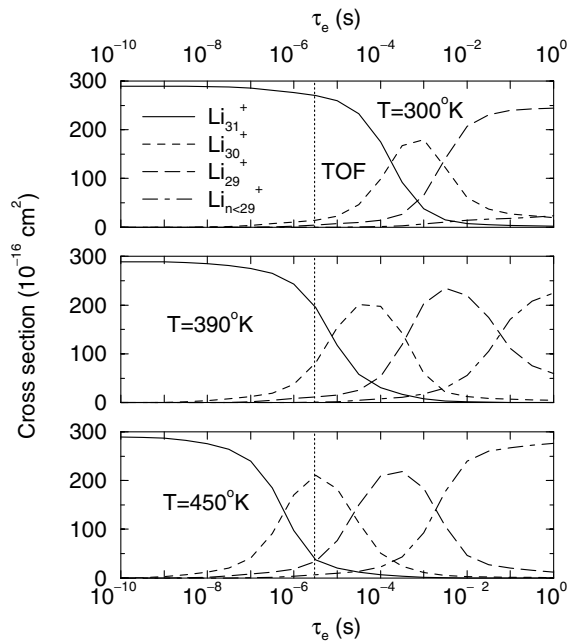
FIG. 4. Calculated cross sections as functions of TOF for three values of temperature. The vertical dotted line indicates the TOF of the present experiment.

confirms that, at 450 K, the dominant fragment is Li_{30}^+, followed by Li_{31}^+ and Li_{29}^+ in almost similar proportions.

The effect of temperature and TOF in the calculated cross sections is illustrated in Fig. 4. This figure shows the variation of the partial cross sections as functions of τ_e for different values of T at a fixed impact energy of 3 keV. For $T = 450$ K and $\tau_e = 3$ μs, the cross sections are those given in Fig. 3 for $E = 3$ keV. Obviously, the choice of different values of T and τ_e is irrelevant for the total CT cross section. However, this is not the case for partial cross sections. It can be clearly seen that, at 450 K, Li_{30}^+ is dominant only in the range $\tau_e \simeq 10^{-6}$–10^{-5} s. For shorter TOF, Li_{31}^+ clusters produced by CT have not enough time to dissociate and, consequently, little evaporation is observed. The opposite occurs for $\tau_e > 10^{-5}$ s. Similar strong variations are observed for different temperatures, but in different ranges of τ_e. A comparison of the results at 300, 390, and 450 K for a fixed value of $\tau_e = 3$ μs shows that evaporation is strongly modified by temperature: while Li_{31}^+ is the dominant species at $T = 390$ K, it has practically disappeared at 450 K [20]. Thus, good agreement between theory and experiment is possible only by using the experimental value of the TOF and a cluster temperature consistent with the experimental distribution. Small deviations from this choice lead to enormous differences in partial cross sections and, therefore, to very different physical interpretations. Similarly, any deficiency in the theoretical treatment may lead to

results in complete disagreement with experiment. For instance, we have checked that exclusion of the collisional energy deposit always leads to Li_{31}^+ as the dominant species, in strong disagreement with experiment.

Now, what about the nonobservable energy deposit δE? δE arises as an intermediate step in the theoretical model. As for transition amplitudes, it depends on impact parameter and exhibits a strong oscillatory behavior (see, e.g., [12]). For an impact energy of 3 keV, it varies between 0 and 3.5 eV, with a mean value of 1.9 eV, which is comparable to the value estimated from experiment.

To conclude, we have presented a combined theoretical and experimental study of CT and evaporation in collisions of slow Li_{31}^{2+} clusters with Cs atoms. We have shown that good agreement between theory and experiment is only possible when the experimental TOF and initial cluster temperature is used in the theoretical modeling. The agreement supports the physical assumptions of our model, in particular, the separation between CT and evaporation, which is justified by the different time scales associated with these processes.

[1] C. Bréchignac et al., Phys. Rev. Lett. **61**, 314 (1988).
[2] U. Saalmann and R. Schmidt, Phys. Rev. Lett. **80**, 3213 (1998).
[3] M. Barat et al., J. Chem. Phys. **114**, 179 (2001).
[4] P. Blaise et al., Phys. Rev. Lett. **87**, 063401 (2001).
[5] D. Babikov et al., J. Chem. Phys. **112**, 7032 (2000).
[6] F. Calvayrac et al., Phys. Rep. **337**, 493 (2000).
[7] M. F. Politis et al., Phys. Rev. A **58**, 367 (1998).
[8] C. Bréchignac et al., Eur. Phys. J. D **12**, 185 (2000).
[9] O. Knospe et al., Eur. Phys. J. D **5**, 1 (1999).
[10] O. Knospe et al., Phys. Rev. A **61**, 022715 (2000).
[11] B. Zarour et al., J. Phys. B **33**, L707 (2000).
[12] P. A. Hervieux et al., J. Phys. B **34**, 3331 (2001).
[13] C. Bréchignac et al., J. Chem. Phys. **101**, 6992 (1994).
[14] C. Klots, J. Chem. Phys. **83**, 5854 (1985); Z. Phys. D **5**, 83 (1987).
[15] C. Bréchignac et al., Phys. Rev. B **49**, 2825 (1994).
[16] C. Bréchignac et al., Eur. Phys. J. D **16**, 91 (2001).
[17] J. Perel and H. L. Daley, *Electronic and Atomic Collisions*, edited by B. C. Cobic and M. V. Kurepa (Institute of Physics, Beograd, Yugoslavia, 1973), Vol. II.
[18] C. B. Alcock et al., J. Phys. Chem. Ref. Data **23**, 385 (1994).
[19] P. A. Hervieux and D. H. E. Gross, Z. Phys. D **33**, 295 (1995); D. H. E. Gross, Phys. Rep. **279**, 119 (1997).
[20] M. Schmidt et al., [Phys. Rev. Lett. **87**, 203402 (2001)] have observed that photofragmentation of Na clusters also depends on T, which allows one to extract caloric curves and study phase transitions.